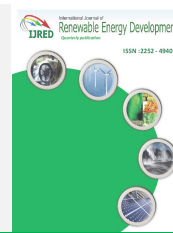




Contents list available at IJRED website

Int. Journal of Renewable Energy Development (IJRED)

Journal homepage: <http://ejournal.undip.ac.id/index.php/ijred>



Research Article

# Poly(vinyl alcohol)-Based Anion Exchange Membranes for Alkaline Direct Ethanol Fuel Cells

Asep Muhamad Samsudin<sup>a,b\*</sup>, Sigrid Wolf<sup>a</sup>, Michaela Roschger<sup>a</sup>, Viktor Hacker<sup>a</sup>

<sup>a</sup> Institute of Chemical Engineering and Environmental Technology, Graz University of Technology, Austria

<sup>b</sup> Department of Chemical Engineering, Diponegoro University, Indonesia

**ABSTRACT.** Crosslinked anion exchange membranes (AEMs) made from poly(vinyl alcohol) (PVA) as a backbone polymer and different approaches to functional group introduction were prepared by means of solution casting with thermal and chemical crosslinking. Membrane characterization was performed by SEM, FTIR, and thermogravimetric analyses. The performance of AEMs was evaluated by water uptake, swelling degree, ion exchange capacity, OH<sup>-</sup> conductivity, and single cell tests. A combination of quaternized ammonium poly(vinyl alcohol) (QPVA) and poly(diallyldimethylammonium chloride) (PDDMAC) showed the highest conductivity, water uptake, and swelling among other functional group sources. The AEM with a combined mass ratio of QPVA and PDDMAC of 1:0.5 (QPV/PDD<sub>0.5</sub>) has the highest hydroxide conductivity of 54.46 mS cm<sup>-1</sup>. The single fuel cell tests with QPV/PDD<sub>0.5</sub> membrane yield the maximum power density and current density of 8.6 mW cm<sup>-2</sup> and 47.6 mA cm<sup>-2</sup> at 57°C. This study demonstrates that PVA-based AEMs have the potential for alkaline direct ethanol fuel cells (ADEFCs) application.

**Keywords:** anion exchange membranes; PVA; PDDMAC; fuel cells; crosslinking.

**Article History:** Received: 28<sup>th</sup> Sept 2020; Revised: 20<sup>th</sup> December 2020; Accepted: 12<sup>th</sup> February 2021; Available online: 18<sup>th</sup> February 2021

**How to Cite This Article:** Samsudin, A.M., Wolf, S., Roschger, M., and Hacker, V. (2021) Poly(vinyl alcohol)-Based Anion Exchange Membranes for Alkaline Direct Ethanol Fuel Cells. *International Journal of Renewable Energy Development*, 10(3), 435-443.

<https://doi.org/10.14710/ijred.2021.33168>

## 1. Introduction

Fuel cells have attracted enormous attention as alternative and highly efficient power generators due to the increasing demand for efficient energy and global environmental issues. The development of proton exchange membrane fuel cells (PEMFCs) has been hindered by several issues, including extensive costs due to the use of a platinum group metal (PGM) catalyst, fuel crossover, sluggish reaction kinetics in an acidic environment and complex water management (Dai *et al.*, 2009; Fang *et al.*, 2015). In order to address these challenges, significant attention has been focused on alkaline fuel cells (AFCs). Since AFCs operate in alkaline conditions and involve the transport of hydroxide ions in place of protons, AFCs offer many advantages compared to PEMFCs. These advantages include the use of lower-cost and non-PGM catalysts, high oxygen reduction rate (ORR), low fuel permeability and higher corrosion resistance of the materials in place under alkaline conditions (Couture *et al.*, 2011; Wang *et al.*, 2013).

AFCs that use ethanol as fuel, the so-called alkaline direct ethanol fuel cells (ADEFCs), can convert the easily storable high-energy fuel virtually emission-free under ambient conditions (Yang *et al.*, 2008).

AEMs are hydroxide ion conductive, separate the cathode from the anode reactants and do not conduct

electrons. AEMs contribute considerably to the performance and efficiency of AFCs (Iraivaninia & Rowshanzamir, 2015).

Poly(vinyl alcohol) (PVA) is an inexpensive polyhydroxy polymer that has remarkable film-forming, non-toxic and hydrophilic properties. PVA has a high density of reactive chemical functional groups that are beneficial for crosslinking and chemical modification. Additionally, due to the high selectivity of water to ethanol, PVA has low ethanol permeability and has the potential to be a backbone polymer for alkaline fuel cells (Susanto *et al.*, 2016).

The AEMs were prepared by dissolving KOH into the matrix of PVA membranes to provide charge carriers. Since KOH has a high solubility in water, however, fuel cells with AEMs of this type are susceptible to conductivity reduction due to the loss of KOH (Xiong *et al.*, 2008). Xiong *et al.* (2008) grafted quaternary ammonium groups onto the PVA matrix to act as charge carriers. When glutaraldehyde (GA) was added directly to the polymer solution, the membrane achieved an ionic conductivity of 7.34 mS cm<sup>-1</sup> at 30 °C. The water uptake was very high, however, resulting in excessive swelling. Du *et al.* (2020) mixed QPVA, poly(diallyldimethylammonium chloride) and GA to form a semi-interpenetrating network. The hydroxide conductivity obtained was 29.1 mS cm<sup>-1</sup> (30°C) with a high swelling volume of 115%. Qiao *et al.* (2012)

\* Corresponding author: [asep.samsudin@tugraz.at](mailto:asep.samsudin@tugraz.at)

compared the direct and indirect chemical crosslinking treatments of PVA/poly(acrylamide-co-diallyldimethylammonium chloride) and showed that indirect crosslinking exhibited both a lower water uptake and swelling degree than direct cross-linking.

In this study, we employed PVA as the main-backbone polymer for AEMs. To convert the PVA membrane into AEMs that conduct hydroxide ions, we used three different approaches: (i) glycidyltrimethylammonium chloride (GTMAC) by quaternization of PVA, (ii) poly(diallyldimethylammonium chloride) (PDDMAC) by blending with PVA and (iii) combination of both techniques. PDDMAC is hydrophilic and environmentally friendly, furthermore it has quaternary ammonium functional groups that can offer OH<sup>-</sup> as charge carriers (Samsudin & Hacker, 2019; Zhang et al., 2013). Moreover, the cyclic structures of PDDMAC demonstrate a considerable steric hindrance, hampering degradation of functional groups by S<sub>N</sub>2 nucleophilic substitution in the alkaline state (Yuan et al., 2018).

To reduce membrane swelling and improve membrane chemical stability, a combination of thermal and indirect chemical cross-linking of the polymer chains with GA-based crosslinker was introduced in the AEMs preparation. The effect of different approaches for inducing ion-conducting functional charges, including types and mass ratios, were investigated and the performance of the best membrane in ADEFCS was examined.

## 2. Materials and methods

### 2.1 Polymers solution preparation

PVA-based AEMs with different ion-conducting sources and mass ratios (Table 1) were prepared. Initially, 10 wt.% PVA aqueous solution was prepared by dissolving PVA (98-99% hydrolyzed, M<sub>w</sub> = 86,000-89,000 g mol<sup>-1</sup>, Sigma-Aldrich) in ultra-pure water at 80°C with stirring.

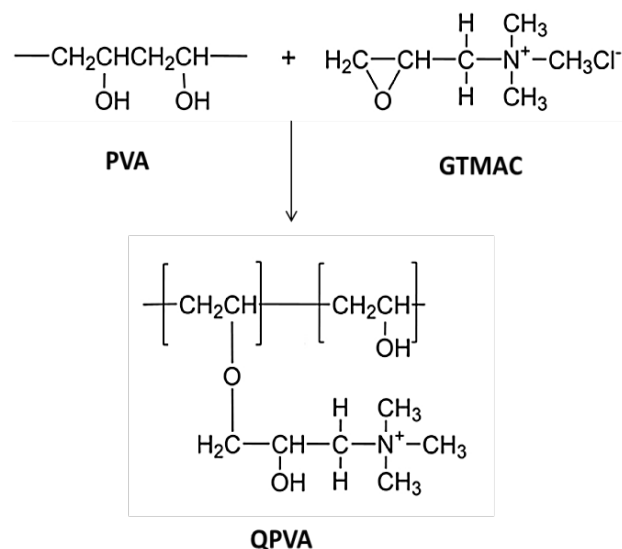


Fig. 1 Reaction scheme of PVA quaternization (Liao et al., 2015).

**Table 1**  
Composition of the samples

Sample names	Description
PVA	10 wt.% PVA
QPVA	10 wt.% QPVA
PV/PDD <sub>0.5</sub>	10 wt.% PVA + 10 wt.% PDDMAC, 1:0.5 mass ratio
QP/PDD <sub>0.5</sub>	10 wt.% QPVA + 10 wt.% PDDMAC, 1:0.5 mass ratio
QP/PDD <sub>0.125</sub>	10 wt.% QPVA + 10 wt.% PDDMAC, 1:0.125 mass ratio
QP/PDD <sub>0.25</sub>	10 wt.% QPVA + 10 wt.% PDDMAC, 1:0.25 mass ratio
QP/PDD <sub>0.375</sub>	10 wt.% QPVA + 10 wt.% PDDMAC, 1:0.375 mass ratio

QPVA was synthesized as reported (Jiang et al., 2018). 5 g PVA was dissolved in 95 mL ultra-pure water at 80°C until obtaining a clear homogeneous solution. Subsequently, a quaternized PVA reaction (Fig. 1) was induced by adding 10 ml of 2.0 M KOH solution (Merck) and 10 g glycidyltrimethylammonium chloride (GTMAC, ≥ 90%, Sigma-Aldrich) to the PVA solution under continuous stirring for 4 h at 65°C. Anhydrous ethanol (Merck) was added to the solution to induce precipitation. The precipitate was then dried at 40°C for 24 h. Lastly, the white QPVA particles obtained were dissolved in ultra-pure water at 80°C with stirring to acquire 10 wt.% QPVA solution.

The PVA solution and the QPVA solution were then blended separately with PDDMAC (M<sub>w</sub> = 20 wt.% in H<sub>2</sub>O, 400,000-500,000, Sigma-Aldrich) while being stirred for 4 hours, resulting in PVA/ PDDMAC and QPVA/ PDDMAC, respectively.

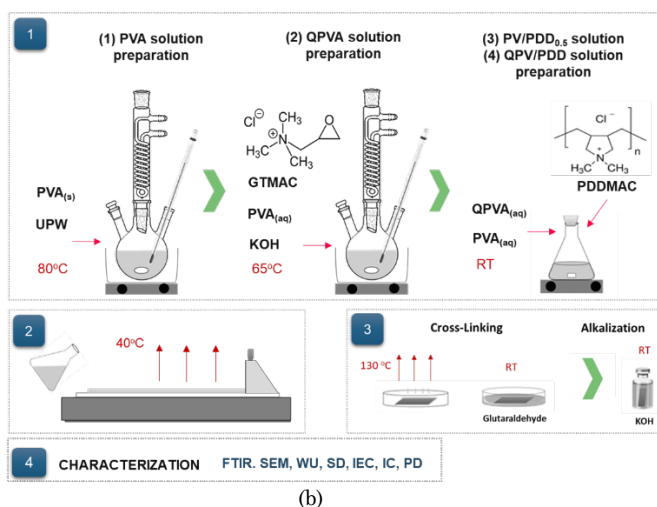
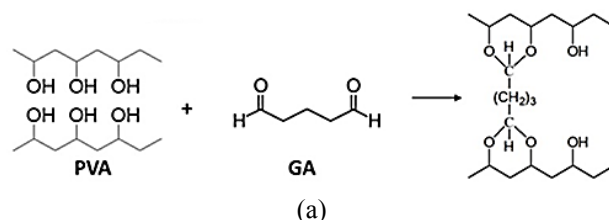


Fig. 2 AEMs preparation method. a) Chemical crosslinking reaction of PVA. b) Schematic of preparation method.

## 2.2 Membrane preparation

The polymer solutions were cast onto the glass substrate with a casting knife (Elcometer 4340 automatic film applicator) and evaporated at 40°C for 24 h then peeled from the glass.

To restrain the swelling tendentious and enhance the mechanical properties of membranes, a thermal and chemical crosslinking combination of the polymer chains was introduced to the membranes. The membranes were annealed at 130°C for an hour to induce physical crosslinking and immersed in a cross-linker solution [10 wt.% glutaraldehyde (GA, Sigma-Aldrich), 0.2 wt.% HCl in acetone solvent] to promote chemical crosslinking between polymer chains (Fig. 2a). Fig. 2b illustrates the procedure of AEMs preparation.

## 2.3 Characterization

### 2.3.1 Structure characterization

The Fourier transform infrared spectroscopy (FTIR) analysis was performed on IR-spectrometer (Bruker ALPHA) to identify the chemical structure of the AEMs. FTIR spectra were obtained in the range of 500 - 4000  $\text{cm}^{-1}$  at 4  $\text{cm}^{-1}$  resolution.

### 2.3.2 Swelling properties

The water uptake (WU) and swelling degree (SD) of the AEMs were determined by measuring the change in weight and dimension of the AEMs before and after immersion in water. Membrane samples were weighted ( $W_d$ ). Additionally, their volume ( $V_d$ ) was measured. Subsequently, the samples were immersed in ultra-pure water at ambient conditions for 24 h. The weight ( $W_w$ ) and volume ( $V_w$ ) of the swelling membranes were measured immediately after eliminating the surface water gently. The WU and SD of the AEMs were calculated by:

$$\text{WU} = \frac{W_w - W_d}{W_d} \times 100\% \quad (1)$$

$$\text{SD} = \frac{V_w - V_d}{V_d} \times 100\% \quad (2)$$

### 2.3.3 Ion Exchange Capacity (IEC)

The ion exchange capacity (IEC) was measured using a back-titration method. The AEM samples were immersed in 1.0 M KOH solution for 24 h to convert the  $\text{Cl}^-$  into the  $\text{OH}^-$  form AEMs. The membranes were then soaked with ultra-pure water for 24 h to remove the KOH residue. Subsequently, the AEMs were equilibrated with a 0.1 M HCl solution for 24 h. The IEC was determined from the reduction in acid quantity. The IEC value was calculated by Equation (3):

$$\text{IEC} = \frac{(V_b - V_m) \cdot C_{\text{HCl}}}{w_d} \quad (3)$$

where  $V_b$  is the consumed NaOH volumes of the blank sample,  $V_m$  is the consumed NaOH volumes of the AEMs,  $C_{\text{HCl}}$  is the concentration of HCl solution, and  $w_d$  is the weight of the dry AEMs.

### 2.3.4 $\text{OH}^-$ conductivity

The  $\text{OH}^-$  conductivity was determined by electrochemical impedance spectroscopy (EIS) using Gamry Reference 600 potentiostat. The membrane samples were alkalized in a 1.0 M KOH solution for 24 h to convert  $\text{Cl}^-$  to  $\text{OH}^-$  in membrane structure. Furthermore, membranes were immersed in ultra-pure water for 24 h to remove the residue of KOH. The samples at a size of  $2.5 \times 1.0$  cm placed into the four-electrode configuration of the conductivity clamp (Bekktch BT110 LLC, Scribner Associates) in ultra-pure water at 30 °C. Impedance was measured over a frequency range of 0.1 Hz–10 kHz (50 mV amplitude). The membrane resistance ( $R_m$ ) was acquired from the intercept of the Nyquist curve with  $Z_{\text{real}}$  axis. The  $\text{OH}^-$  conductivity was calculated, as stated by equation 4.

$$\sigma = \frac{d}{R_m \cdot T \cdot W} \quad (4)$$

where  $d$ ,  $T$ , and  $W$  are the distance of the electrodes, the thickness, and width of the membranes, respectively. The results were compared with the commercial membrane Fumasep FAA3 (Fuma-Tech)

### 2.3.4 Thermal stability

Thermogravimetric analysis was carried out using a STA 449 C apparatus (NETZSCH). The membrane samples were placed on the alumina sample holder. Measurements were performed by heating from 25 to 600°C, under  $\text{N}_2$  atmosphere at a heating rate of 10 °C  $\text{min}^{-1}$ .

### 2.3.5 Single-cell performance test

The fuel cell performance of the PVA-based AEMs was investigated using the alkaline direct ethanol single cell test (ADEFC). The membranes were immersed in 1 M KOH for 24 h and cleaned with ultrapure water before the cell test was performed. Electrodes were prepared by depositing ink slurries of the anode/cathode catalysts on the gas diffusion layer (GDL) using an automatic ultrasonic spray coater (Sonotek, USA). The catalyst ink was prepared by mixing a 7:3 ratio of 2-propanol and ultrapure water containing 30 wt% of an anion exchange ionomer (fumion® FAA-3 solution in NPM, 10 %).

The anode was fabricated by spraying the ink slurry of a PdNiBi/C catalyst synthesized by the modified instant reduction method (Cermenek *et al.* 2020) on carbon cloth (ELAT - Hydrophilic Plain Cloth, thickness of 0.406 mm, fuel cell store). Meanwhile, ink slurry of a commercial PtRu/C catalyst (Platinum, nominally 40 %, Ruthenium, nominally 20% on carbon black, HiSPEC® 10000) was sprayed onto a carbon paper as GDL (Sigracet 29 BC, thickness of 0.235 mm, fuel cell store) to produce the cathode. The electrode preparation resulted in a metal loading of 0.75  $\text{mg cm}^{-2}$  for the anode and 0.5  $\text{mg cm}^{-2}$  for the cathode.

The membrane electrode assembly (MEA) of 2 cm x 2 cm was prepared by assembling the AEM between the cathode and anode. The MEAs were carefully assembled in a self-made ADEFC. A constant flow rate of oxygen gas (5.0, 99.995 %, 25  $\text{mL min}^{-1}$ ) was used as a cathode feed gas, whereas a mixture of 1 M ethanol in 1 M KOH was applied as anode fuel (5  $\text{mL min}^{-1}$ ). The measurements were conducted at ambient temperature for QPV/PDD<sub>0.5</sub> and FAA3 AEMs as reference. Measurements were also performed at higher temperatures (36°C, 44°C, 53°C, and

57°C) to investigate the temperature dependence. The current densities (I) and cell potentials (V) of the single cells were determined using a Reference 600TM Potentiostat (Gamry instruments). The results were plotted in a current density – potential (I-V) graphic including an additional curve for the power density.

### 3. Results

#### 3.1 Chemical structure

The FTIR spectra of PVA, QPVA, PVA/PDD<sub>0.5</sub>, and QPV/PDD<sub>0.5</sub> are compared in Figure 3 in order to identify the main functional groups that exist in AEMs structures. The main PVA-based peaks were detected at around 3328, 2923, 1651, 1412, 1320, 1089, and 836 cm<sup>-1</sup>. These peaks are recognized as the -OH stretching, C-H stretching, amines, CH<sub>2</sub> stretching, C-O carbonyl stretching, a further additional -OH stretching and C-H bending vibration.

From Fig. 3, We can observe the decrease in peak height at 3328 cm<sup>-1</sup> in QPVA and QPV/PDD<sub>0.5</sub> spectra. This indicates a reduction in the concentration of OH-groups in the PVA chain due to the reaction with GTMAC during the quaternization (Müller *et al.*, 2017). Furthermore, the increase in peak intensity can be seen around 1651 cm<sup>-1</sup> by order of PVA, QPVA, PV/PDD<sub>0.5</sub>, and QPV/PDD<sub>0.5</sub>. This is possibly due to the increase of quaternary ammonium groups owing to the quaternization of PVA, the introduction of PDDMAC, and the combination of quaternization and PDDMAC addition, respectively. This can be confirmed from the increase in hydroxide conductivity in Fig 8a.

Figure 4 illustrates a proposed model of the chemical structure of PV/PDD, and QPV/PDD AEMs according to the FTIR spectra and the literature (Du *et al.*, 2020; Samsudin & Hacker, 2019). The physical crosslinking between PVA or QPVA chains are formed by heat treatment (annealing). The heat treatment creates hydrogen bonding between -OH groups of PVA or QPVA chains, facilitating crosslinking to establish three-dimensional structures (MirafTAB *et al.*, 2015). The chemical cross-linker promotes covalent bonding between the -CHO groups of GA and the -H groups of PVA, which form a C-O-C bond. The PDDMAC is trapped into the crosslinked PVA or QPVA network as a distinct semi-interpenetrating polymer network.

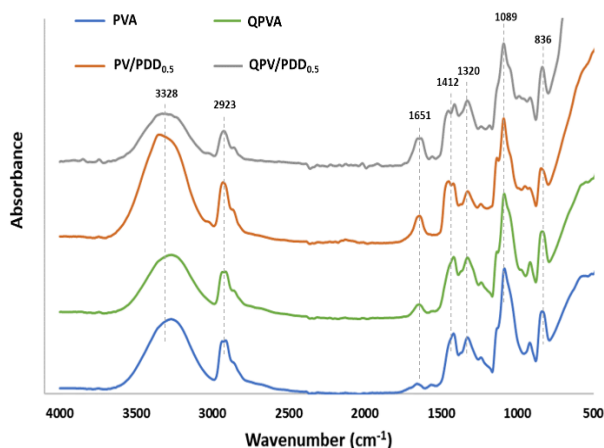


Fig. 3 FTIR spectra of PVA-based AEMs.

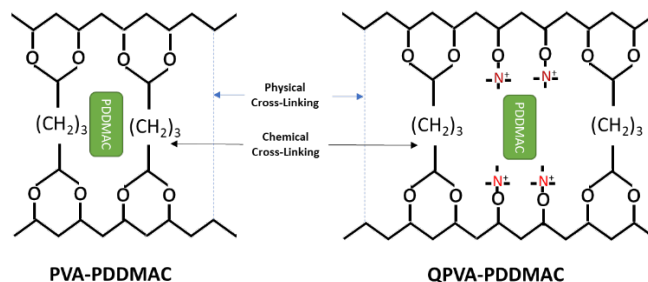


Fig. 4 Model of the chemical structure of PVA/PDD and QPV/PDD AEMs.

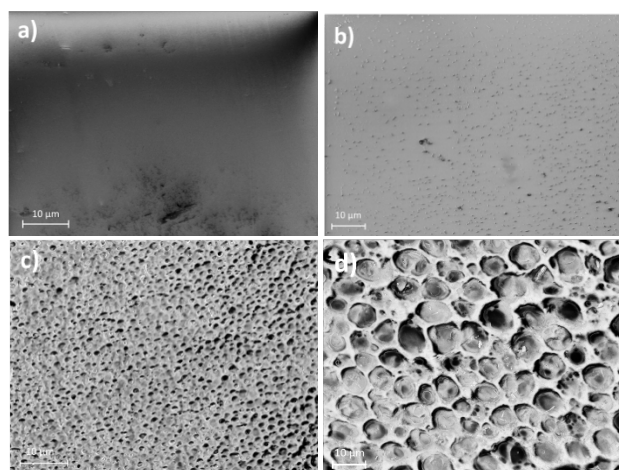


Fig. 5 SEM images of PVA-based AEMs. a) Pristine PVA, b) QPVA, c) PVA/PDD<sub>0.5</sub>, d) QPV/PDD<sub>0.5</sub>.

Table 2

Physicochemical parameters of PVA-based AEMs.

Membranes	IEC (meq·g <sup>-1</sup> )	WU (%)	SD (%)	$\sigma$ (mS·cm <sup>-1</sup> )
PVA	0.74	10	18	1.09
QPVA	1.07	13	25	2.50
PV/PDD <sub>0.5</sub>	1.53	35	45	23.03
QP/PDD <sub>0.5</sub>	2.05	55	51	54.46
QP/PDD <sub>0.125</sub>	1.44	23	36	9.66
QP/PDD <sub>0.25</sub>	1.57	34	40	28.49
QP/PDD <sub>0.375</sub>	1.77	43	47	42.04
FAA3	-	-	-	24.59

#### 3.2 Morphology

The surface morphologies of various PVA-based AEMs are depicted in Fig. 5. SEM image of pristine PVA membrane (Fig. 5a) depicts a smooth and homogeneous surface indicating no phase separation. On the other hand, QPVA AEM (Fig. 5b) shows a relatively clear image with small dots spread on the membrane surface. These dots are probably due to the influence of quaternary ammonium moiety on the PVA polymer structure (Hari Gopi & Bhat, 2018).

Interesting results can be seen in Fig. 5c and Fig 5d, which exhibit the surface SEM images of PV/PDD<sub>0.5</sub>, and QPV/PDD<sub>0.5</sub>, respectively. PV/PDD<sub>0.5</sub> image shows a rough surface with small lump-like structures distributed evenly. This apparently occurred because a typical interaction between PVA and PDDMAC leads to phase

separation. On the QPV/PDD<sub>0.5</sub> membrane, the heterogeneous structure is more pronounced. The phase separation on the AEM resembles a honeycomb structure. The interconnected parts would appear to be QPVA chains connected to each other as a result of crosslinking. The central part is the PDDMAC and this combination forms a semi-interpenetrating polymer network structure (semi-IPN) (Bai *et al.*, 2018). This structure can enhance the membrane flexibility and water-holding capacity, while also expanding the bulk of the membrane, thus providing more space for hydroxide transport in the membrane (Samsudin & Hacker, 2019). These results can support the model proposed in Fig 4.

### 3.3 Water uptake

AEMs need a sufficient water content in order to be adequate hydroxide conductors. Water clusters inside the AEMs offer beneficial transport passages for hydroxide ions, and thus increasing the OH<sup>-</sup> conductivity (Zhang *et al.*, 2013). Due to the constant thermal crosslinking temperature and the unchanging concentration of chemical crosslinking, the water uptakes can rely only on exchangeable quaternary ammonium groups (Hari Gopi & Bhat, 2018).

Figure 6a demonstrates the water uptake (WU) of the AEMs with different cation sources. Pure PVA has the lowest WU of all AEMs sample types because this membrane has no exchangeable quaternary ammonium groups. The QPVA possesses higher water uptake in contrast to the pure PVA membrane. This is owing to the quaternization process of PVA from GTMAC. Exchangeable quaternary ammonium groups become presented in the chemical structure that leads to enhancement of the water uptake of the membrane. On PV/PDD<sub>0.5</sub>, the source of the cation groups was from PDDMAC, resulting in higher WU compared to QPVA. This could be due to the higher ion-exchange capacity of PDDMAC than QPVA. QV/PDD<sub>0.5</sub> acquired the highest water uptake of content in comparison with other membrane types. This result is as expected because these AEMs combined two different sources of exchangeable cation functional groups.

Water uptake (WU) of the QPVA/PDDMAC AEMs with different mass-ratio can be observed from Fig. 6b. It can be seen that WU shows a linear rise with the increase of PDDMAC to the QPVA mass ratio. Higher PDDMAC content leads to the higher ion exchange capacity of AEMs, increasing water uptake.

### 3.4 Swelling degree

Despite the presence of a certain quantity of water in the AEMs is required for conducting OH<sup>-</sup>, excessive water uptake might provoke a severe swelling of the membrane. This extreme swelling can reduce the dimensional stability and possibly hinders the preparation of membrane electrode assembly (MEA) by obstructing contact between the active layer of the electrodes and the AEMs (Feketeföldi *et al.*, 2016). The swelling degree (SD) of different PVA-based AEMs was evaluated in the interest of evaluating any change in the membrane dimensions. Figure 7a exhibits the SD of the AEMs with various ion-exchange sources. The SD of pristine PVA AEMs is 18% and increases with the order QPVA, PVA/PDD<sub>0.5</sub>, and QPV/PDD<sub>0.5</sub>. The increase in SD is proportional to the rise of WU membranes.

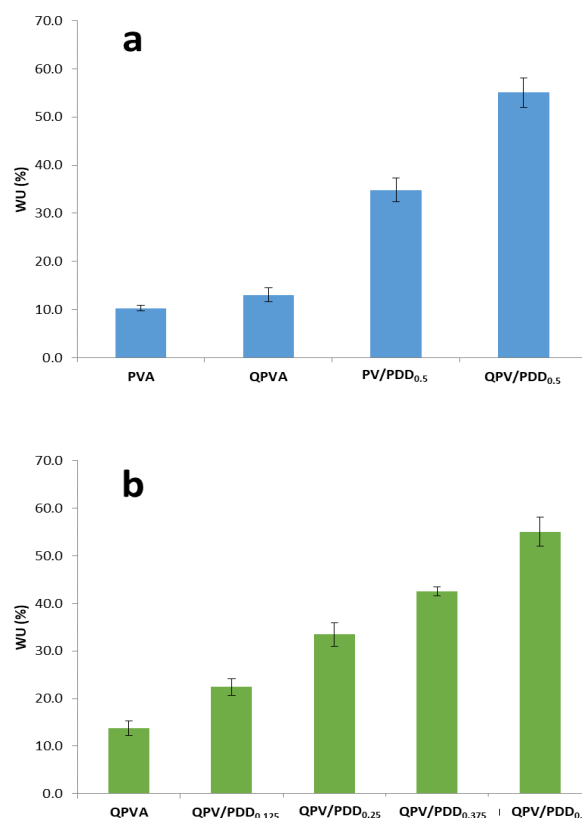


Fig. 6 Water uptake of AEMs. a) different cation sources, b) different mass ratio of PDDMAC.

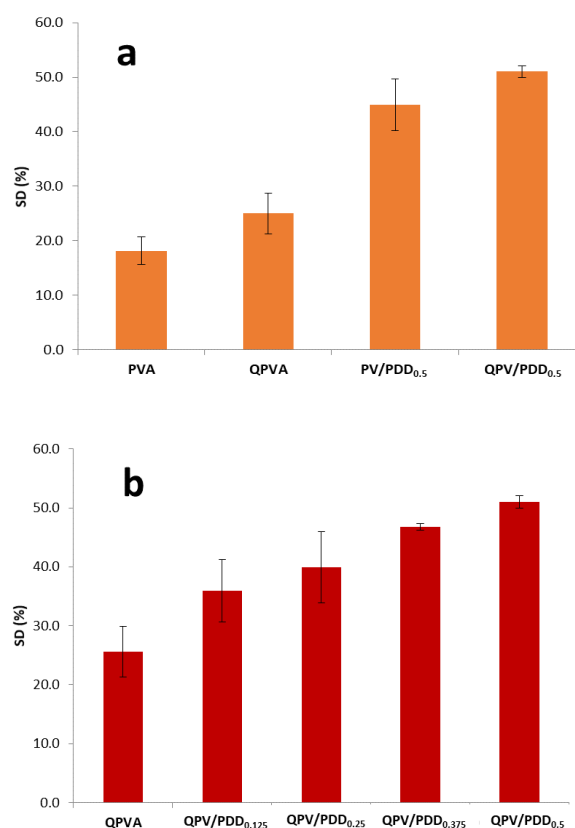


Fig. 7 Swelling degree of AEMs. a) different cation sources, b) different mass ratio of PDDMAC.

The swelling degree (SD) of the QPVA/PDDMAC AEMs with different mass-ratio can be seen from Fig. 7b. It can be observed that SD rises linearly with the increase of PDDMAC to the QPVA mass ratio. Higher PDDMAC content leads to a proportionally higher ion exchange capacity in AEMs and increasing water uptake leads to alteration in the membrane dimension. QPV/PDD<sub>0.5</sub> AEMs possess the highest SD of 51%.

### 3.5. Ion exchange capacity

Ion exchange capacity (IEC), an important parameter of the AEMs, denotes the quantity of ion-exchangeable groups in the AEMs, which is essential for the OH<sup>-</sup> conductivity (Qiao *et al.*, 2012). Fig. 8a and Table 2 show the ion exchange capacity of the AEMs with various ion-exchange sources at room temperature. The IEC increases with the order PVA, QPVA, PVA/PDD<sub>0.5</sub>, and QPV/PDD<sub>0.5</sub>.

Figure 8b illustrates the ion exchange capacity of the QPVA/PDDMAC AEMs with different mass-ratios at room temperature. With the increasing content of PDDMAC, the IEC value of the membrane rises. QPV/PDD<sub>0.5</sub> AEMs possess the highest SD of 2.05 meq.g<sup>-1</sup>. A higher IEC value can increase the OH<sup>-</sup> conductivity of the membrane.

### 3.6 Hydroxide conductivity

Hydroxide conductivity ( $\sigma$ ) plays the most critical attributes of AEMs. This parameter strongly determines the performance of AEFs. Typically, the OH<sup>-</sup> conductivity of AEMs is highly dependent on the number of quaternary ammonium groups present in the AEMs, water uptake, and membrane morphology.

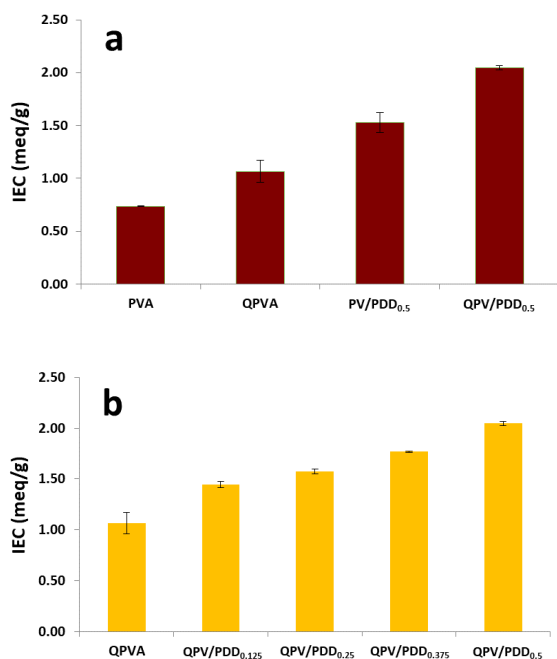


Fig. 8 Ion exchange capacity of AEMs. a) different cation sources, b) different mass ratio of PDDMAC.

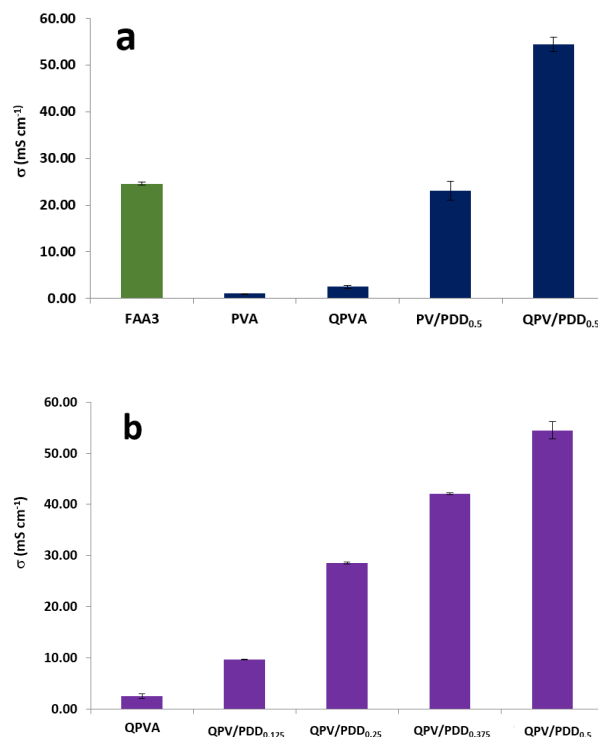


Fig. 9 OH<sup>-</sup> conductivity of AEMs. a) different cation sources, b) different mass ratio of PDDMAC.

Figure 9a depicts the OH<sup>-</sup> conductivity of AEMs. Pristine PVA AEMs have the lowest conductivity of 1.09 mS cm<sup>-1</sup> owing to no exchangeable quaternary ammonium groups existing in the membrane. PVA undergoing quaternization (QPVA) slightly possesses increases the conductivity of the AEMs to 2.5 mS cm<sup>-1</sup>. This is probably because the quaternary ammonium groups present in PVA chemical structure are not high. In order to enhance the number of quaternary ammonium groups in the AEMs, the GTMAC quantity should be increased in the quaternization step. Nevertheless, excessive concentration of quaternary ammonium groups could weaken the mechanical strength of the membranes due to excessive swelling or brittleness attributable to an intensive dryness (Merle *et al.*, 2011). PV/PDD<sub>0.5</sub> and QPV/PDD<sub>0.5</sub> AEMs result in much higher OH<sup>-</sup> conductivity of 23.03 mS cm<sup>-1</sup> and 54.46 mS cm<sup>-1</sup>, respectively. The rise of OH<sup>-</sup> conductivity is in ratio with the increase of WU membranes. These results confirm that the OH<sup>-</sup> conductivity of AEMs is relies to a great extent on the WU of membranes and PDDMAC contributed more to the number of quaternary ammonium groups available in the membrane. A combination of QPVA and PDDMAC results in the highest OH<sup>-</sup> conductivity of AEMs. Interestingly, the OH<sup>-</sup> conductivity of QPV/PDD<sub>0.5</sub> is much higher than the sum of conductivity for QPVA and PV/PDD<sub>0.5</sub>. This phenomenon is still not well understood, probably due to good compatibility between QPVA and PDDMAC polymers.

OH<sup>-</sup> conductivity of the QPVA/PDDMAC AEMs with different mass-ratios can be observed from Fig. 9b. The ionic conductivity of AEMs has an incline to the QPVA mass ratio along with the rise of PDDMAC. Higher

PDDMAC content leads to the higher ion exchange capacity of AEMs, which in turn increases conductivity. QPV/PDD<sub>0.5</sub> AEMs possess the highest conductivity of 54.46 mS cm<sup>-1</sup> which is 2.2 times higher than the commercial AEM FAA3.

### 3.6 Thermal stability

Figure 10 depicts the TGA curves for PVA, QPVA, QPV/PDD<sub>0.5</sub>, and QPV/PDD<sub>0.5</sub> AEMs, respectively. The TGA curve of the pristine PVA membrane displays three major weight loss steps. The first step at a temperature of 30–105 °C is owing to the evaporation of the discharge of water molecules in the membrane and moisture absorbed from the atmosphere. The second step at around 237–330 °C is because of the degradation of the PVA polymer membrane. The third step at around 351–444 °C is due to the cleavage backbone of the PVA polymer membrane.

Fig. 10 also shows the TGA curve of QPVA membrane. The QPVA membrane displays three major weight loss steps as well. The first step at a temperature of 30–98 °C is thanks to the evaporation of the discharge of water molecules in the membrane and moisture absorbed from the atmosphere. The second step at around 294–356 °C is as a consequence of the degradation of the QPVA polymer membrane. The third step at around 371–460 °C is due to the cleavage of the C–C bond of the QPVA polymer membrane (Yang *et al.*, 2010).

The TGA curve of the PV/PDD<sub>0.5</sub> membrane in Fig. 10 also shows three major weight loss steps. The first step at a temperature of 30–105 °C is also attributable to the evaporation of the discharge of water molecules in the membrane and moisture absorbed from the atmosphere. The second step at around 258–325 °C is potentially due to the decomposition of quaternary ammonium cationic groups, the crosslinking bridges cleavage, and the breaking of some C–O and C–C bonds from PDMAC and PVA (Zhou *et al.*, 2019). The third step at 356–470 °C is associated with the PVA and PDDA decomposition polymer backbones.

Furthermore, the TGA curve of QPV/PDD<sub>0.5</sub> AEMs illustrates three major weight loss steps. The first step at 30–90 °C is as a result of the evaporation of the discharge of water molecules in the membrane and moisture absorbed from the atmosphere.

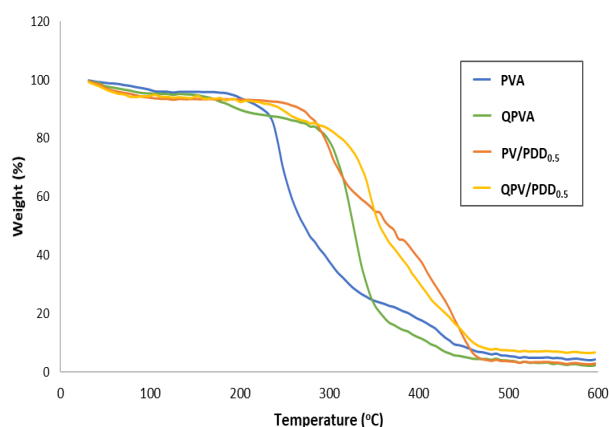


Fig. 10 TGA curves of AEMs.

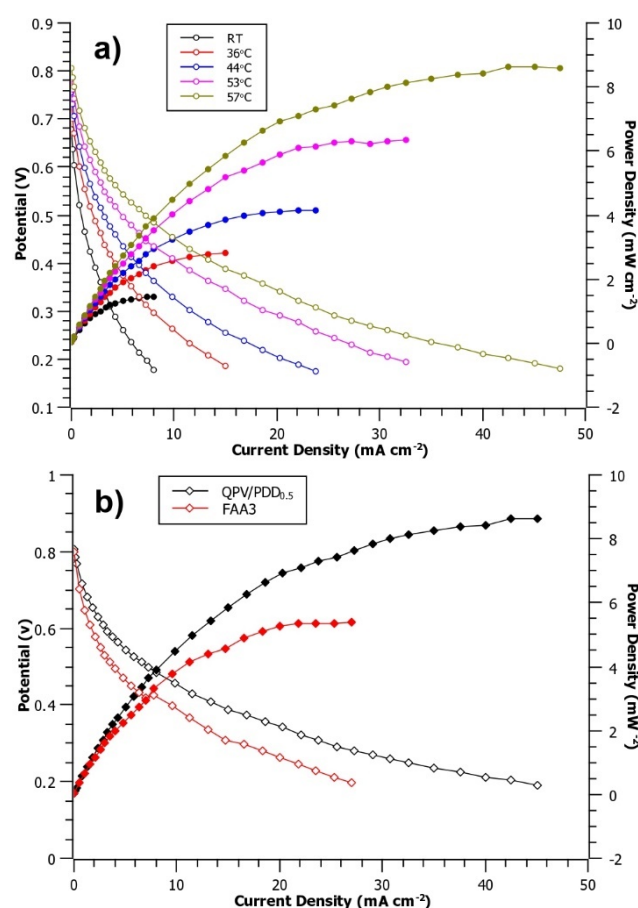


Fig. 11 Power density (filled symbols) and polarization curves (open symbols) of QPV/PDD<sub>0.5</sub> AEMs. a) different temperature, b) comparison with FAA3 at 57 °C.

The second step at around 250–335 °C is possibly on account of the quaternary ammonium cationic groups decomposition, the crosslinking bridges cleavage, and the breaking of some C–O and C–C bonds from PDDMAC and QPVA. The third step at 356–480 °C is caused by the PVA and PDDMAC decomposition polymer backbones. Therefore, the TGA analysis results confirm the sufficient thermal stability of membranes for the low-temperature ADEFCs application.

### 3.7 Single cell performance

The QPV/PDD<sub>0.5</sub> membrane, which gives the highest OH<sup>-</sup> conductivity, was used to fabricate MEA. The membrane performance in fuel cells was determined in alkaline direct ethanol single test cells. The effect of temperature on AEM performance was investigated. The commercial FAA3 membrane was also used to prepare MEA for a comparison.

Figure 11a shows typical ADEFC I–V (left axis, open symbols) and I–P (right axis, filled symbols) plots of the QPV/PDD<sub>0.5</sub> membrane. The cell voltage and the maximum power density of all samples increased with ascending temperatures. This corresponds to a similar study (Liao *et al.*, 2015) which is attributed to the improved reaction kinetics at the electrodes and conductivity of the cell at higher temperatures. The MEAs fabricated with QPV/PDD<sub>0.5</sub> membrane showed a maximum peak power density of 8.6 mW cm<sup>-2</sup> at a current

density of 47.6 mA cm<sup>-2</sup> at 57°C. Figure 11b depicts a comparison of QPV/PDD<sub>0.5</sub> and FAA3 membrane performances at 57°C. It is noted that under the same measuring conditions, the MEA fabricated with FAA3 showed a maximum peak power density of 5.4 mW cm<sup>-2</sup> at a current density of 27.0 mA cm<sup>-2</sup>, which is lower than that the QPV/PDD<sub>0.5</sub> membrane. These results are also in agreement with the higher OH<sup>-</sup> conductivity of QPV/PDD<sub>0.5</sub> than FAA3.

#### 4. Conclusion

Anion exchange membranes (AEMs) composed of poly(vinyl alcohol) (PVA) as a backbone polymer and different approaches for introducing ion-exchange functional groups have been successfully prepared by a solution casting method. A combination of QPVA and PDDMAC polymer shows better conductivity than other AEMs types. Ion conductivity, water uptake, and swelling degree of AEMs rise with the increase of PDDMAC to PVA mass ratio. The AEMs showed excellent thermal stability at high degradation temperatures above 250 °C. QPV/PDD<sub>0.5</sub> AEM achieved the highest hydroxide conductivity of 54.46 mS cm<sup>-1</sup>. The performance of ADEFC with QPV/PDD<sub>0.5</sub> AEMs showed a maximum power density of 8.6 mW cm<sup>-2</sup> with a current density of 47.6 mA cm<sup>-2</sup> at 57 °C and is thus higher than that of commercially available FAA3 membranes under the same measuring conditions. These results demonstrate that the PVA-based AEMs have the potential for application in alkaline direct ethanol fuel cells.

#### Acknowledgments

This work was supported by the Austrian Science Fund (FWF) project no. I 3871-N37 and the Indonesia-Austria Scholarship Programme (IASP).

#### References

Bai, H., Li, Z., Zhang, S., Wang, W., & Dong, W. (2018). Interpenetrating polymer networks in polyvinyl alcohol/cellulose nanocrystals hydrogels to develop absorbent materials. *Carbohydrate Polymers*, 200(August), 468–476. <https://doi.org/10.1016/j.carbpol.2018.08.041>

Couture, G., Alaaeddine, A., Boschet, F., & Ameduri, B. (2011). Polymeric materials as anion-exchange membranes for alkaline fuel cells. *Progress in Polymer Science*, 36(11), 1521–1557. <https://doi.org/10.1016/j.progpolymsci.2011.04.004>

Dai, W., Wang, H., Yuan, X., Martin, J. J., & Yang, D. (2009). A review on water balance in the membrane electrode assembly of proton exchange membrane fuel cells. *International Journal of Hydrogen Energy*, 34(23), 9461–9478. <https://doi.org/10.1016/j.ijhydene.2009.09.017>

Du, X., Zhang, H., Yuan, Y., & Wang, Z. (2020). Semi-interpenetrating network anion exchange membranes based on quaternized polyvinyl alcohol/poly(diallyldimethylammonium chloride). *Green Energy and Environment*. <https://doi.org/10.1016/j.gee.2020.06.015>

Fang, J., Wu, Y., Zhang, Y., Lyu, M., & Zhao, J. (2015). Novel anion exchange membranes based on pyridinium groups and fluoroacrylate for alkaline anion exchange membrane fuel cells. *International Journal of Hydrogen Energy*, 40(36), 12392–12399. <https://doi.org/10.1016/j.ijhydene.2015.07.074>

Feketeföldi, B., Cermenek, B., Spirk, C., Schenk, A., Grimmer, C., Bodner, M., Koller, M., Ribitsch, V., & Hacker, V. (2016). Chitosan-Based Anion Exchange Membranes for Direct Ethanol Fuel Cells. *Journal of Membrane Science & Technology*, 06(01), 1–9. <https://doi.org/10.4172/2155-9589.1000145>

Hari Gopi, K., & Bhat, S. D. (2018). Anion exchange membrane from polyvinyl alcohol functionalized with quaternary ammonium groups via alkyl spacers. *Ionics*, 24, 1097–1109. <https://doi.org/10.1007/s11581-017-2272-x>

Iravaninia, M., & Rowshanzamir, S. (2015). Polysulfone-based Anion Exchange Membranes for Potential Application in Solid Alkaline Fuel Cells. *Journal of Renewable Energy and Environment*, 2(2), 59–65.

Jiang, X., Sun, Y., Zhang, H., & Hou, L. (2018). Preparation and characterization of quaternized poly(vinyl alcohol)/chitosan/MoS<sub>2</sub> composite anion exchange membranes with high selectivity. *Carbohydrate Polymers*, 180(October 2017), 96–103. <https://doi.org/10.1016/j.carbpol.2017.10.023>

Liao, G. M., Yang, C. C., Hu, C. C., Pai, Y. L., & Lue, S. J. (2015). Novel quaternized polyvinyl alcohol/quaternized chitosan nano-composite as an effective hydroxide-conducting electrolyte. *Journal of Membrane Science*, 485, 17–29. <https://doi.org/10.1016/j.memsci.2015.02.043>

Merle, G., Wessling, M., & Nijmeijer, K. (2011). Anion exchange membranes for alkaline fuel cells: A review. *Journal of Membrane Science*, 377(1–2), 1–35.

Mirafteb, M., Saifullah, A. N., & Çay, A. (2015). Physical stabilisation of electrospun poly(vinyl alcohol) nanofibres: comparative study on methanol and heat-based crosslinking. *Journal of Materials Science*, 50(4), 1943–1957. <https://doi.org/10.1007/s10853-014-8759-1>

Müller, F., Andretta, R., de Oliveira Meneguzzi, L., & Arthur Ferreira, C. (2017). Development of quaternized poly(vinyl alcohol) anion-exchange membranes for applications in electrodialysis. *Journal of Applied Polymer Science*, 134(31), 1–9. <https://doi.org/10.1002/app.44946>

Qiao, J., Fu, J., Liu, L., Liu, Y., & Sheng, J. (2012). Highly stable hydroxyl anion conducting membranes poly(vinyl alcohol)/poly(acrylamide-co-diallyldimethylammonium chloride) (PVA/PAADDA) for alkaline fuel cells: Effect of cross-linking. *International Journal of Hydrogen Energy*, 37(5), 4580–4585. <https://doi.org/10.1016/j.ijhydene.2011.06.038>

Samsudin, A. M., & Hacker, V. (2019). Preparation and characterization of PVA/PDDA/nano-zirconia composite anion exchange membranes for fuel cells. *Polymers*, 11(9). <https://doi.org/10.3390/polym11091399>

Susanto, H., Samsudin, A. M., Faz, M. W., & Rani, M. P. H. (2016). Impact of post-treatment on the characteristics of electrospun poly(vinyl alcohol)/chitosan nanofibers. *AIP Conference Proceedings*, 1725. <https://doi.org/10.1063/1.4945541>

Wang, Y.-J., Qiao, J., Baker, R., & Zhang, J. (2013). Alkaline polymer electrolyte membranes for fuel cell applications. *Chemical Society Reviews*, 42(13), 5768–5787. <https://doi.org/10.1039/c3cs60053j>

Xiong, Y., Fang, J., Zeng, Q. H., & Liu, Q. L. (2008). Preparation and characterization of cross-linked quaternized poly(vinyl alcohol) membranes for anion exchange membrane fuel cells. *Journal of Membrane Science*, 311(1–2), 319–325. <https://doi.org/10.1016/j.memsci.2007.12.029>

Yang, C. C., Chiu, S. J., Chien, W. C., & Chiu, S. S. (2010). Quaternized poly(vinyl alcohol)/alumina composite polymer membranes for alkaline direct methanol fuel cells. *Journal of Power Sources*, 195(8), 2212–2219. <https://doi.org/10.1016/j.jpowsour.2009.10.091>

Yang, C. C., Chiu, S. J., Lee, K. T., Chien, W. C., Lin, C. T., & Huang, C. A. (2008). Study of poly(vinyl alcohol)/titanium oxide composite polymer membranes and their application on alkaline direct alcohol fuel cell. *Journal of Power Sources*, 184(1), 44–51. <https://doi.org/10.1016/j.jpowsour.2007.12.029>

- <https://doi.org/10.1016/j.jpowsour.2008.06.011>
- Yuan, Y., Shen, C., Chen, J., & Ren, X. (2018). Synthesis and characterization of cross-linked quaternized chitosan/poly(diallyldimethylammonium chloride) blend anion-exchange membranes. *Ionics*, 24(1173), 1180. <https://doi.org/10.1007/s11581-017-2280-x>
- Zhang, J., Qiao, J., Jiang, G., Liu, L., & Liu, Y. (2013). Cross-linked poly(vinyl alcohol)/poly (diallyldimethylammonium chloride) as anion-exchange membrane for fuel cell applications. *Journal of Power Sources*, 240, 359–367. <https://doi.org/10.1016/j.jpowsour.2013.03.162>
- Zhou, T., Wang, M., He, X., & Qiao, J. (2019). Poly(vinyl alcohol)/Poly(diallyldimethylammonium chloride) anion-exchange membrane modified with multiwalled carbon nanotubes for alkaline fuel cells. *Journal of Materiomics*, 5(2), 286–295. <https://doi.org/10.1016/j.jmat.2019.01.012>



© 2021. This article is an open access article distributed under the terms and conditions of the Creative Commons Attribution-ShareAlike 4.0 (CC BY-SA) International License (<http://creativecommons.org/licenses/by-sa/4.0/>)